

# Asynchronous Execution of Heterogeneous Tasks in AI-coupled HPC Workflows

Vincent R. Pascuzzi<sup>1</sup>, Matteo Turilli<sup>1,2</sup>, Shantenu Jha<sup>1,2</sup>

<sup>1</sup> Brookhaven National Laboratory, Upton, NY 11973, USA

<sup>2</sup> Rutgers, the State University of New Jersey, Piscataway, NJ 08854, USA

**Abstract**—Heterogeneous scientific workflows consist of numerous types of tasks and dependencies between them. Middleware capable of scheduling and submitting different task types across heterogeneous platforms must permit asynchronous execution of tasks for improved resource utilization, task throughput, and reduced makespan. In this paper we present an analysis of an important class of heterogeneous workflows, viz., AI-driven HPC workflows, to investigate asynchronous task execution requirements and properties. We model the degree of asynchronicity permitted for arbitrary workflows, and propose key metrics that can be used to determine qualitative benefits when employing asynchronous execution. Our experiments represent important scientific drivers, are performed at scale on Summit, and performance enhancements due to asynchronous execution are consistent with our model.

**Index Terms**—hpc, workflow, adaptability, machine learning, artificial intelligence

## I. INTRODUCTION

Scientific discovery increasingly requires sophisticated and scalable workflows. Introducing AI/ML models into traditional high performance computing (HPC) workflows has been an enabler of highly accurate modeling, and a promising approach for significant scientific advances [1]. These workflows often comprise hundreds to thousands of heterogeneous tasks [2]. Those tasks have diverse dimensions of heterogeneity: **implementation** (e.g., executables or function/methods in an arbitrary language), **resource requirements** (e.g., executing on CPUs and/or GPUs, computational or data intensive operations), and **duration** (e.g., from less than a second to many hours; size, from a core to many cores over one or more compute nodes). Specifically, for AI/ML driven HPC workflows, alongside traditional CPU, GPU and, possibly, multi-node MPI tasks, AI/ML usually requires the execution of high-throughput function calls, often implemented in an interpreted language such as Python.

Typically, in AI/ML driven HPC workflows, simulation tasks generate data, and ML tasks use that data for training or inference, while inference results are used to guide the next set of simulations [3], [4], creating a dependence between the two types of task. A naive approach in which all the simulations run before the ML, or all simulations pause while inference (or training) is ongoing, leads to poor resource utilization (e.g., while the ML tasks run, a large amount of the allocated HPC resource idles). Further, continuous learning, surrogate re-training, and optimal execution of campaigns are becoming increasingly important and prevalent, making the concurrent

and asynchronous execution of simulations and ML phases of the workflow unavoidable, and BSP-like hard temporal separation of simulations and ML phases untenable.

As a consequence, the middleware that manages the execution of the workflow application has to be able to concurrently schedule, place and execute simulations and ML tasks, viz., MPI executables alongside Python functions with wildly varying execution lifetimes — the former for hours, the latter for as little as fractions of seconds. For the task-execution middleware to do so, in a way that maximizes resource utilization while minimizing the workflow makespan, requires it to explicitly support asynchronous execution of heterogeneous tasks. Resource utilization and efficiency depend upon the specifics of each workflow, workload mix (i.e., type of tasks, and their individual properties), and how effectively the task-execution middleware manages the heterogeneity of the tasks and resources.

In this paper, we focus on the resource management challenge from having to execute tasks with diverse resource requirements. We discuss conditions for asynchronous execution, and offer a quantitative basis and experimental characterization of the improvements it can bring in terms of resource utilization and task throughput, and thus makespan. We offer four main contributions: (1) an asynchronous implementation of DeepDriveMD [4], [5] — a framework to execute ML-driven molecular-dynamics workflows on HPC platforms at scale; (2) a performance evaluation of asynchronous DeepDriveMD; (3) a model of asynchronous behavior; and (4) a general performance evaluation of that model for workflows with a varying degree of asynchronous execution.

In §II we discuss several AI-driven HPC workflows and workflow systems, as generalized motivation and importance of asynchronous execution. In §III, we define asynchronous execution and its relationship with data and control flow when designing a workflow application. We present in §IV conditions for workflows-level asynchronicity and the concept of task execution time masking, which together can be used to estimate the expected relative improvement in adopting asynchronous execution pattern with respect to sequential execution for arbitrary workflows. In §V we formalize the notion of asynchronous execution by modeling its behavior and performance for the metrics of task throughput and resource utilization. In §VI we compare synchronous and asynchronous execution of DeepDriveMD, measuring the benefits of the latter. We then generalize those results, offering an exper-

imental characterization of the performance gains provided by different degrees of heterogeneity for a given workflow. Finally, in §VII we discuss the implications of our model and performance analysis for the design of workflow applications with heterogeneous tasks, when executed on HPC resources.

## II. RELATED WORK

Asynchronicity spans multiple levels of an HPC stack and affects many areas of a distributed execution. Asynchronous execution, communication and coordination are implemented and leveraged in many runtime systems, both to distribute workload among executors and/or coordinate the messaging among executing processes. Uintah [6], Charm++ [7], HPX [8], Legion [9], and PaRSEC [10] are all examples of runtime using asynchronicity to coordinate execution.

Contrary to the runtime system listed above, in this paper we specifically focus on asynchronous execution for AI-enabled workflows, in which we have different types of tasks. We assume tasks to be black boxes and therefore, in our modeling, we abstract away the details of asynchronous communication as data dependencies are assumed to be satisfied, either before or during execution. From an engineering perspective, our study contributes to the analysis of applications developed, not only for DeepDriveMD and RADICAL-Cybertools, but also for systems like Parsl [11], Swift/T [12], or myriad workflow engines that manage the potentially asynchronous execution of heterogeneous workflows.

Significant examples of AI-driven HPC workflows solutions include Colmena [3], Mummi/Merlin [13], [14], [15], and Proxima [16]. Each of these workflow solutions and supported applications involves running a time-varying heterogeneous mix of HPC and AI/ML tasks.

Further examples of AI-driven HPC workflow can be found in Refs. [17], [18] both of which use DeepDriveMD Ref. [5], [4] to couple ML and molecular dynamic simulations. The performance characterization of DeepDriveMD established that, when feasible, asynchronous execution of ML and simulation tasks can improve both resource utilization and task throughput. Nonetheless, the implementation of such an execution model depends on specific capabilities of the task utilized and cannot be applied to all task types executed via DeepDriveMD.

## III. DESIGNS AND IMPLEMENTATIONS

Computationally, HPC workflows often require the adoption of two task execution paradigms: control-flow and data-flow. In the control-flow paradigm, executing a workflow requires explicit control over distinct task instances. Each task launches with an input dataset, performs a bounded amount of computation on that input, and exits execution. In the data-flow paradigm, workflow execution is defined in terms of data dependencies among tasks, establishing what data each task has to share with another task.

Design-wise, control and data flows paradigms are not mutually exclusive. Workflow engines can independently manage data staging, inter-task communication, task execution and task processing. Task data requirements, i.e., that a task can start

processing only when certain input data are available, can be equally satisfied by diverse designs: (1) Staging input data before executing a task; or, (2) Communicating (*e.g.*, streaming or sending a message with a data location) the input data to the task when that task is already executing. Note that executing a task is different from having that task starting to process input data: a task can be executing but also idle.

Workflows can benefit from the concurrent use of both control and data flows when they require executing heterogeneous tasks. Some of those tasks may have to communicate their input data to each other, or may idle while waiting for input data to be available. Other tasks may instead be launched only when data are already available and terminated after those data have been processed. For example, a certain type of tasks (*e.g.*, MPI simulations) may occupy so many resources that it would be too costly keeping them executing while idling. Inversely, some other types of task (*e.g.*, ML inference) may require limited and specialized resources like GPUs, execute frequently and for only few seconds and thus be too costly to launch and terminate every time they need to run.

In this paper, we explore the design space of control and data flows by modeling asynchronous execution. A workflow execution is asynchronous when multiple tasks of **different types independently and concurrently execute** on the available resources. A task executes independently when it does not need to coordinate with other tasks to proceed its execution.

Note that independence here pertains to task that are executing, not to the dependency among tasks before their execution. For example, a task may depend on data produced by another task but, when executing, those data are already available and thus their availability does not require coordination among executing tasks. In this context, it is crucial to distinguish between tasks that are *running* and those that are *executing*. When running, a task is not necessarily performing any useful calculation as it may be idling (*i.e.*, wasting resources) until triggered to do so. Instead, an executing task is necessarily performing useful work that advances the workflow to its goal.

Asynchronous execution should not be confused with ‘asynchronous data staging’ or the more common ‘asynchronous communication’. The former indicates that each task’s input data is staged independently; the latter that communications among sender and receiver do not need to be coordinated. Independent tasks may require staged files or asynchronously communicate but, in this paper, we abstract those details, focusing on modeling and characterize asynchronous execution as defined above.

Exemplars in Refs. [17], [18], [4] require a general purpose approach to asynchronous task execution in DeepDriveMD. Such an approach should not depend on the specific implementation of each task, remain agnostic towards the communication and data capabilities of each task and make no assumptions about streaming capabilities. DeepDriveMD must account for tasks that have to be executed sequentially, those that can concurrently execute and communicate or exchanging data, and those that have no relationship and can be executed either concurrently or sequentially.

We extended DeepDriveMD [4] to implement asynchronous executions of heterogeneous workflows. DeepDriveMD can now manage an arbitrary number of task types, each requiring arbitrary amount of CPU cores and/or GPUs. Each task or each type can be fully independent, dependent on the output of another task or dependent on communicating with one or more other tasks. DeepDriveMD can be configured to execute tasks concurrently or sequentially, taking into account their dependency constraints. As with the previous version, DeepDriveMD is implemented as a thin layer on top of the RADICAL-EnsembleToolkit (EnTK) workflow engine. EnTK keeps tracks of task dependences and submits them for execution to RADICAL-Pilot, a pilot system designed to execute heterogeneous workloads on HPC platforms.

#### IV. CONDITIONS FOR WORKFLOW-LEVEL ASYNCHRONICITY

We argue there exist two conditions for workflow-level asynchronicity (WLA): (1) inter-task dependencies and (2) resource availability. As detailed below, these conditions, in addition to task execution time (TX), dictate resource utilization and task throughput, two key metrics that determine the total time to execution (TTX, or makespan) when employing asynchronous task execution. The importance of considering only executing and not running tasks must be stressed as a running task will increase resource utilization but will not progress a workflow to completion.

##### A. Condition I: Inter-Task Dependencies

When representing a workflow as a directed acyclic graph (DAG), asynchronous task execution only applies to workflows which contain one or more forks with diverging paths that do not eventually converge. As such, given enough resources, independent tasks of different types can execute concurrently.

Representing a workflow as a DAG allows one to visualize dependencies (edges) between tasks (nodes). Figure 2 shows four DAGs representative of four distinct workflows with various levels of inter-task dependence. Task set indices are ordered breadth-first. The lower bound on the degree of asynchronicity ( $DOA_{dep}$ ), permitted by task dependencies, arises when the DAG is sequential, *e.g.*, a linear chain, Fig. 1a for which  $DOA_{dep} = 0$ . The upper bound, *i.e.*, completely asynchronous, arises a DAG whose edge set is the empty set such as that in Fig. 1d where  $DOA_{dep} = n$ . In between these bounds, asynchronicity in general varies as a function of the number of forks with diverging paths that do not rejoin.

##### B. Condition II: Task Resource Requirements

Assuming unlimited resources, inter-task dependency is, in principle, the condition for determining the degree of asynchronicity for a given workflow. For example, the DAG in Fig. 1d has  $DOA_{dep} = n$ , so in the case of infinite resources, each of the  $n + 1$  task sets' tasks can execute asynchronously. In practice, however, resources are limited, and therefore an additional condition based on the available (allocated) resources must be imposed.

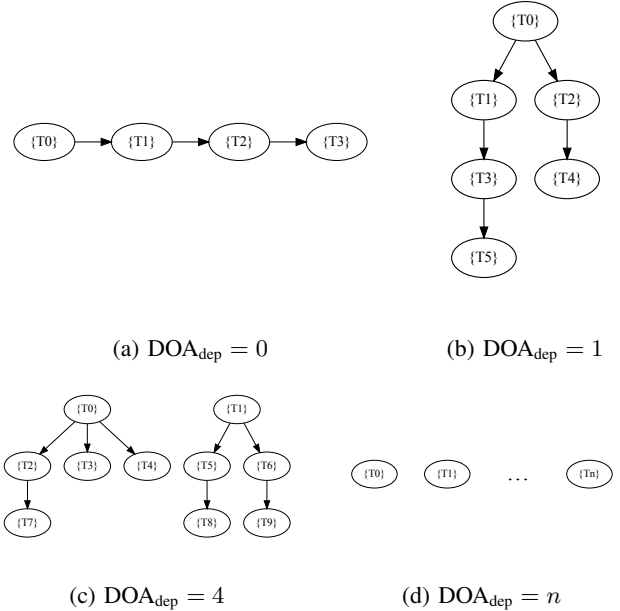


Fig. 1: Abstract directed acyclic graphs and their respective task dependency degree of asynchrony,  $DOA_{dep}$ . These are abstract in the sense that only task sets (nodes), their orderings (indices) and dependencies (edges) are given. These DAGs contain no information about the number of tasks in each task set, their resource requirements, task execution time (TX), *etc.* Task set indices are ordered in a breadth-first manner.

To describe the resource-permitted degree of asynchronicity,  $DOA_{res}$ , consider again the workflow DAG in Fig. 1d. Let  $\tilde{R}$  be the set of all allocated resources and  $\cup_i R_i$  be the set resources required to asynchronously execute the  $n + 1$  task sets. Complete asynchronicity is achieved if and only if  $\cup_i R_i \subseteq \tilde{R}$ , in which case  $DOA_{res} = DOA_{dep} = n$ . On the other extreme, if  $R_i = \tilde{R} \forall_i$ , then we have two possibilities: (1) execute each task set in arbitrarily or based on a given scheduler's heuristics (since the execution of the full set of tasks from any task set requires 100% of the allocated resources); or (2) execute from two or more task sets the subsets such that  $\cap_i R_i = \tilde{R}$ . Despite  $DOA_{res} = 0$  in the first case and  $DOA_{res} > 0$  in the second, there exists an equivalence between the two wherein the latter effectively is the collapse of a dependency-free DAG to a chain as in Fig. 1a. This scenario highlights how haphazard attempts to adopt asynchronicity into a workflow will not always yield any benefit for the workflow as a whole, and instead can lead to significant loss of development time during the design process.

Richer, albeit more complex, situations lie between the two extremes. Take, for example, the workflow DAG of Fig. 1c, which has  $DOA_{dep} = 4$ . Depending on the resource requirements for each of  $T_2 - T_9$  task sets,  $0 \leq DOA_{res} \leq 5$ . As such, we define,

$$WLA \equiv \min[DOA_{dep}, DOA_{res}] \quad (1)$$

to quantify the asynchronicity permitted by the workflow.

### C. Task Execution Time and Masking

A primary motivation for asynchronous task execution is to improve resource utilization which is directly correlated with task throughput. However, examples have already been given that reveal the introduction of asynchronicity does not guarantee increased task throughput, specifically when the majority of upstream tasks (ancestors) dominate resource use. On the other hand, when resource requirements endow a workflow with a  $\text{DOA}_{\text{res}} > 0$  and it is possible to exploit TX, the overall workflow TTX can be reduced; in other words, one can achieve higher task throughput.

Leveraging TX can afford *masking*, a technique wherein longer running tasks effectively ‘hide’ contributions from shorter running tasks’ a workflow’s TTX. To illustrate masking, consider the workflow DAG of Fig. 1b for which  $\text{DOA}_{\text{dep}} = 1$ . Assume the allocated resources are such that once  $T_0$  completes, the chains  $\{T_1, T_3, T_5\}$  and  $\{T_2, T_4\}$  can execute asynchronously; then  $\text{DOA}_{\text{res}} = \text{DOA}_{\text{dep}} = 1$ . For concreteness, further assume the following TTX assignments:

$$t_0 = 500\text{s}, t_1 = t_2 = 1000\text{s}, 2t_3 = 2t_5 = t_4 = 4000\text{s}.$$

To demonstrate the utility of masking, we begin with a purely sequential workflow using the PST model, where the DAG represents a pipeline, each rank corresponds to a stage, and each task set to tasks. In the sequential model, the TTX is given by,

$$t^{\text{Seq}} = \sum_i t_i + C, \quad (2)$$

where  $C$  is a constant representing the workflow management system’s overheads such as communications. In general,  $C$  is negligible with task execution times  $O(10)$  minutes and larger. As such, we disregard small overheads in future calculations but consider them in later analyses. Plugging into Eqn. 2 the above assigned TX values, the sequential TTX is  $t^{\text{Seq}} = 7500\text{s}$ .

We now demonstrate how the workflow TTX can be significantly reduced by exploiting the conditions for asynchronicity and the parameters of the workflow; specifically here,  $\text{WLA} = \min(\text{DOA}_{\text{dep}}, \text{DOA}_{\text{res}}) = 1$  and the TX assignments. First, the WLA enables asynchronous execution of the chains  $H_1 \equiv \{T_1, T_3, T_5\}$  and  $H_2 \equiv \{T_2, T_4\}$ . Second, the TX assignments lead to masking such that the contribution from task set  $T_5$  to the workflow TTX is hidden by the execution of task set  $T_4$  since  $t_4 = t_3 + t_5$  and the corresponding task sets now execute asynchronously. In general, the asynchronous TTX for an asynchronous workflow is given by,

$$\begin{aligned} t^{\text{Async}} &= \sum_{i < j} t_i + \max[t_{H_j}] \\ &\leq t^{\text{Seq}}, \end{aligned} \quad (3)$$

where the sum is over the sequential task sets and  $j$  corresponds to the task set with the smallest index within the rank where one more asynchronicity-permitting forks occur (in this case,  $j = 1$ ). We have equality if and only if  $t_{H_j} = t_{H_k} \forall_{j,k}$ .

Asynchronous execution of the workflow under discussion therefore has a TTX of  $t_0 + t_{H_1} = 5500\text{s}$ . We define the relative improvement as,

$$I \equiv 1 - \frac{t^{\text{Async}}}{t^{\text{Seq}}}, \quad (4)$$

for which, in this example, gives roughly a 26% reduction compared to the sequential execution. This example makes clear the potential gains when a workflow is designed to leverage WLA as well as TX masking.

## V. EXPERIMENTS

We design three workflows (experiments) to characterize asynchronous task execution performance and to compare with their respective sequential workflow. All workloads use the *stress* application for their tasks and, for simplicity, omit operations such as data movement and staging which are largely platform-dependent. The use of an artificial workload enables precise setting of TX and makes judicious use of shared allocations while alleviating overheads (*e.g.*, inputs, configurations, *etc.*) involved when using application-specific executables. As we focus on workflow asynchronicity, this approach permits analysis without loss of generality.

### A. DeepDriveMD

DeepDriveMD [4] comprises four types of tasks—Simulation, Aggregation, Training, and Inference—as described earlier. All task but Aggregation are heterogeneous, *i.e.*, both CPUs and GPUs, and the number of each type of task and their execution times vary among task sets. Table I details the workflow parameters which are scaled appropriately with respect to the number of nodes used for these studies.

There exist dependencies between the different task sets (*c.f.*, Fig. 1a); Simulation tasks are responsible for producing the data that is consumed by Aggregation tasks, the aggregated data is then inputted to ML model Training tasks, and lastly Inference tasks perform inference using the trained models. As such, a single iteration of this workflow necessarily needs to be sequential in terms of the execution of various tasks. In practice, however, ML training and inference typically require multiple iterations (sufficient data volumes) for convergence and to reach some level of accuracy or precision in terms of their predictions. It is therefore possible and, as will be demonstrated, advantageous to asynchronously execute tasks of different types among iterations while also ensuring dependencies are met.

Each task set can execute concurrently, *e.g.*, all Simulation tasks run at the same time, each task set is executed sequentially, as described previously. As such, sequential execution of this workflow uses a single pipeline to orchestrate task execution, where each stage executes sequentially and spawns at least one task that receives input from a preceding one. To construct an asynchronous workflow from multiple (three) independent chains, we use

Task Set	CPU cores/Tasks	GPUs/Tasks	# Tasks ( $\times 3$ )	TX ( $\pm 0.05\sigma$ ) [s]
Simulation	4	1	96	340
Aggregation	32	0	16	85
Training	4	1	1	63
Inference	16	1	96	38

TABLE I: DeepDriveMD workflow tasks. The TX for each task was extracted from Ref. [4] and scaled down by a factor of four. A variable offset  $0.05\sigma$  is added to TX of each task to mimic the stochastic behavior of actual executables.

the equivalent DAG shown in Fig. 2a<sup>1</sup>, where task sets are staggered. Using the PST nomenclature, the complete DAG corresponds to a single pipeline, each rank to a stage, and each task set to the tasks comprising the workload. Task specifications for this workflow are given in Table I.

### B. Abstract-DAG

Two additional workflows are constructed from a single arbitrary abstract DAG. Figure 2b shows the DAG considered for these studies, which consists of eight task sets labelled T0–T7 and dependencies among them.

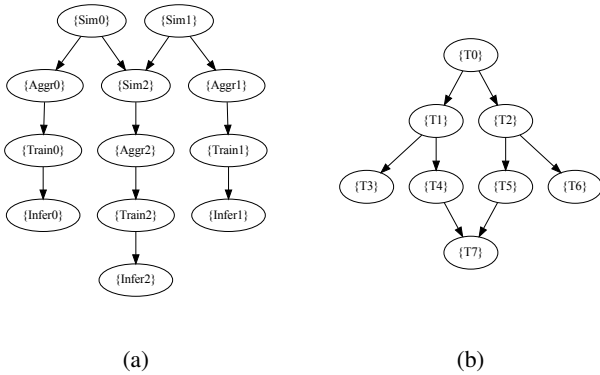


Fig. 2: Directed acyclic graphs corresponding to (a) DeepDriveMD and (b) arbitrary workflows.

Two concrete workflows based on the abstract DAG, denoted c-DAG1 and c-DAG2, are considered to support the conditions for WLA, and to quantify the degree to which asynchronicity is permitted by a specific workflow instantiation. Both concrete workflows are assigned task sets with an arbitrary number of tasks, resources and TX; see Table II.

Task properties are chosen for each concrete workflow to explore two distinct use-cases from a single abstract DAG, and how different parameters can affect the relative improvement when incorporating asynchronicity.

## VI. PERFORMANCE CHARACTERIZATION

We evaluate the achievable level of asynchronicity, resource utilization and time-to-solution for several artificial workloads

<sup>1</sup>An alternative DAG representation of this workflow is three independent chains, one for each iteration. However, this would not admit asynchronous execution as defined in §III.

executing on Oak Ridge National Laboratory’s Summit super-computer. Summit has roughly 4600 Power9 SMT4<sup>2</sup> compute nodes each with six NVIDIA V100 GPUs interconnected via NVLink, and a peak application performance of 200 PF. In these studies, we use a total of 16 nodes for each experiment, giving 706 CPU compute cores and 96 GPUs.

To characterize and evaluate the performance of our designs presented in §V, we construct synthetic workloads representative of real-world workflow applications. For example, we consider workloads comprising a combination of homogeneous and heterogeneous tasks, and different types of tasks whose TX vary among different tasks with dependencies between them. To calculate the relative improvement,  $I$  (Eqn. 4), for each experiment we execute both sequential and asynchronous modes. We impose a TTX constraint on c-DAG1 and c-DAG2; the sequential TTX is about 2000 s for both.

Results for asynchronous executions are summarized at the end of this section, in Table III.

### A. DeepDriveMD

The DeepDriveMD workflow is in principle purely sequential: Simulation  $\rightarrow$  Aggregation  $\rightarrow$  Training  $\rightarrow$  Inference. As such, the workflow TTX is bounded below by the level of asynchronicity permitted by the number of times it is executed. Inspection of the DAG in Fig. 2a reveals the workflow (each task set) is executed three times, and three independent chains beginning at rank 1 means  $DOA_{\text{dep}} = 2$ . Based on task requirements in Table I, the allocated resources give  $DOA_{\text{res}} = 1$ . Hence,  $WLA = 1$  for this workflow.

Figure 3 shows the CPU and GPU resource utilization for three iterations of the DeepDriveMD workflow as a function of TTX, with white-space representing resources on which there are no executing tasks and colored regions representing utilized resources. Comparing Fig. 5a and Fig. 5b, sequential and asynchronous execution, respectively, it is clear the allocated resources are far better utilized with asynchronicity. The improved use of resources naturally leads to a higher task throughput, as shown by the decrease in the asynchronous workflow TTX. From Eqn. 2, with the TX values from Table I, sequential execution has a TTX of approximately  $3t^{\text{Seq}} = 1578$  s, the leading factor a result of the workflow being executed three times. The independent chain in the asynchronous workflow DAG with the largest combined TX is the chain with task set {Sim2} as the top-level ancestor,

<sup>2</sup>The SMT4 variant has 24 cores per processor, and each Summit node comprises two such processors, for a total of 48 cores per node. Two cores per processor are dedicated to operation, leaving 44 compute cores per node.

Task Set	CPU cores/Task	GPUs/Task		# Tasks ( $\times 3$ )		Mean TTX Fraction	
		c-DAG1	c-DAG2	c-DAG1	c-DAG2	c-DAG1	c-DAG2
T0	16	1	1	96	96	0.38	0.19
{T1, T2}	40	0	0	32	32	0.11	0.08
{T3, T6}	4	0	1	16	96	0.06	0.38
{T4, T5}	32	1	1	16	16	0.08	0.12
T7	4	1	0	96	16	0.36	0.23

TABLE II: Summary of the abstract DAG workflow tasks for the concrete DAGs ‘c-DAG1’ and ‘c-DAG2’. Similar task types are assigned the same resources and their respective task sets are grouped within braces. The task set TX values are sampled from a normal distribution  $\mathcal{N}(\mu, \sigma = 0.05)$ , where  $\mu = (\text{Mean TTX Fraction} \times 2000 \text{ [s]})$  to emulate stochastic behavior of actual executables; these fractions have been rounded to two significant figures in the table.

giving  $t_H = t^{\text{Seq}} = 526 \text{ s}$ . Task sets {Sim1}, {Sim2}, and the three Inference task sets, each requiring all 96 GPUs, are ineligible for asynchronicity due to insufficient resources. Then, plugging into Eqn. 3 the values  $2t_{\text{Sim}0} = 2t_{\text{Sim}1} = 680 \text{ s}$ ,  $3t_{\text{Infer}0} = 3t_{\text{Infer}1} = 3t_{\text{Infer}2} = 114 \text{ s}$  and  $t_H$ , the asynchronous workflow execution time is calculated to be  $t^{\text{Async}} = 1320 \text{ s}$ , yielding  $I = 0.17$ .

Important to note is the discrepancy of about 4% between the calculated  $t^{\text{Async}}$  and measured value of 1373 s. This can be attributed to two key facts: (1) corresponding to roughly half the disagreement is we disregard constant overheads in the EnTK framework (the constant factor  $C$  in Eqn. 2), and (2) Eqn. 3 assumes infinite resources. Since each Inference task set requires all available resources, we have the scenario described in Sec. IV-B where the otherwise independent chains collapse to a single chain dependent on the resource allocation.

In light of the TTX disagreement between theory and practice for this multi-iteration workflow, an alternative formulation for calculating  $t^{\text{Async}}$  can be used:

$$t^{\text{Async}} = nt^{\text{Seq}} - (n-1)t_{\text{Aggr}} - (n-2)t_{\text{Train}}. \quad (5)$$

such that  $n-1$  ( $n-2$ ) sets of Aggregation (Training) tasks can be executed concurrently across iterations. Equation 5 makes clear that TX-masked tasks do not contribute to the overall TTX (they are subtracted away). Thus, unlike Eqn. 3, Eqn. 5 correctly does not mask  $t_{\text{Infer}}$  due to resource constraints. It will be useful in later analysis to generalize this equation as,

$$t^{\text{Async}} = \sum_{k=0}^{-1+n} t_k(-k+n). \quad (6)$$

In the DeepDriveMD workflow, Simulation tasks have sufficiently large TX such that Aggregation and Training tasks can both be masked, *i.e.*,  $t_{\text{Sim}2} > t_{\text{Aggr}0} + t_{\text{Train}0} = t_{\text{Aggr}1} + t_{\text{Train}1}$ . Substituting the respective values into Eqn. 5, the estimated TTX is 1345 s, a difference of 2% with respect to the measured TTX the remaining. This remaining time is attributed to the constant overheads from the framework, visible in Fig. 3 as white-space between task set executions.

### B. c-DAG1

The task property assignments in c-DAG1 were chosen to demonstrate a case when asynchronicity has a negative

impact on a workflow’s TTX and task throughput. The workflow is represented by the DAG in Fig. 2b, which has  $\text{DOA}_{\text{dep}} = \text{DOA}_{\text{res}} = 2$  for  $\text{WLA} = 2$ . As such, the workflow permits asynchronicity, however, the task requirements, given in Table II, prevent an improvement in resource utilization and therefore task throughput.

This is due to the fact that, while it is possible to run together task sets  $\{T_3, T_6\}$  and  $\{\{T_4, T_5\}, T_7\}$ , the relatively small TX of  $\{T_3, T_6\}$  and  $\{T_4, T_5\}$ , as well as dependencies for  $\{T_7\}$  to begin executing, offer a negligible improvement with TX masking. Indeed, the additional overheads—roughly 2% of the workflow TTX—induced by introducing asynchronicity here result in a larger TTX than that of the sequential execution. Direct application of Eqn. 3 yields a predicted asynchronous TX of 1860 s, which disagrees with the measured TX by just under 6%: 4% of the difference accounted for by earlier arguments from the DeepDriveMD example, and a nearly 2% performance hit for overheads incorporating asynchronicity. Accounting for this difference, Eqn. 4 can be used to estimate the potential gains, giving  $I = 0.01$ , which does not provide motivation to adopt asynchronicity. Using the measured values of the sequential and asynchronous versions of this workflow,  $I = -0.015$ ; asynchronicity indeed has a negative relative improvement. Therefore, workflow’s with similar traits to c-DAG1 are preferentially sequential.

### C. c-DAG2

We demonstrate last a concrete workflow from the abstract DAG in Fig. 2b. Let us take the proposed approach of first predicting the relative improvement for this workflow using the relevant task parameters from Table II for c-DAG2. From earlier analyses, we can anticipate an under-estimate of 4–6% using Eqn. 3. Plugging in the task execution times, the predicted TTX of this workflow is calculated to be 1300s. Assuming an under-estimate, we account for a 6% discrepancy with the measured TTX to give 1378 s. From Eqn. 2, the predicted TTX of the sequential execution of c-DAG2 is 2000 s. The estimated relative improvement is thus  $I = 0.31$ , suggesting the workflow will benefit from asynchronicity. Experimentation measures sequential and asynchronous execution TX of 1856 s and 1372 s, respectively, for  $I = 0.26$ . The non-zero  $\text{DOA}_{\text{dep}}$  and  $\text{DOA}_{\text{res}}$ , which imply a  $\text{WLA} > 0$ , as well as the agreement between the predicted and measured asynchronous TX, guarantee an asynchronicity advantage.

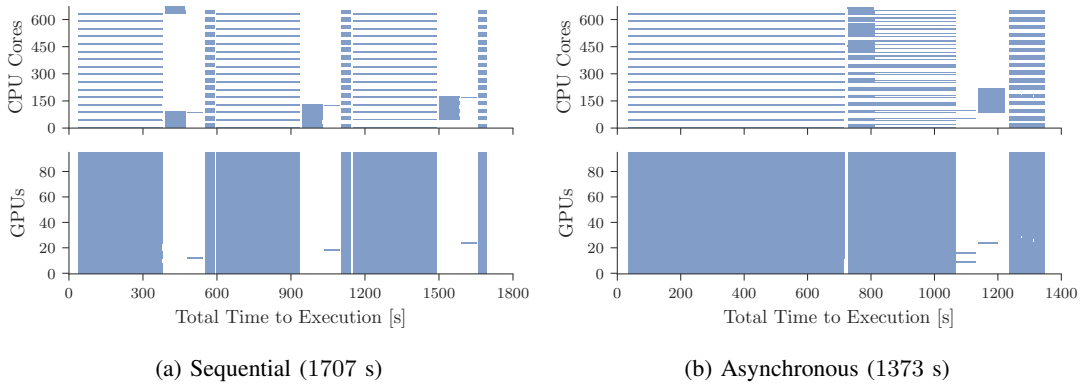


Fig. 3: Three iterations of DeepDriveMD workflow, with sequential (left) and asynchronous (right) execution. The TTX improvement achieved with asynchronicity is about 20%.

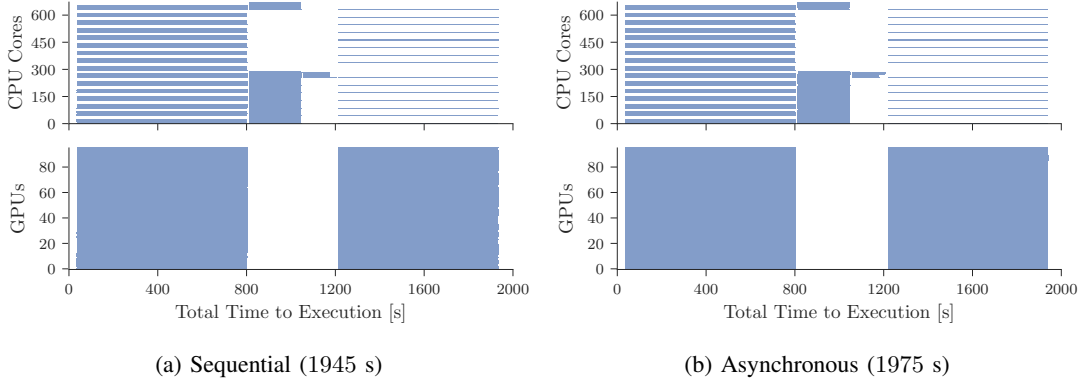


Fig. 4: Resource utilization for workflow c-DAG1. Sequential (left) and asynchronous (right) execution. Due to the small TX (6% and 7%) of the task sets permitting asynchronous execution ( $\{T_3, T_6\}$  and  $\{\{T_4, T_5\}, T_7\}$ ), and additional overheads in spawning multiple workflow executions required for asynchronicity, resource utilization and task throughput improvements are negligible, ultimately resulting in a negative value of  $I$ .

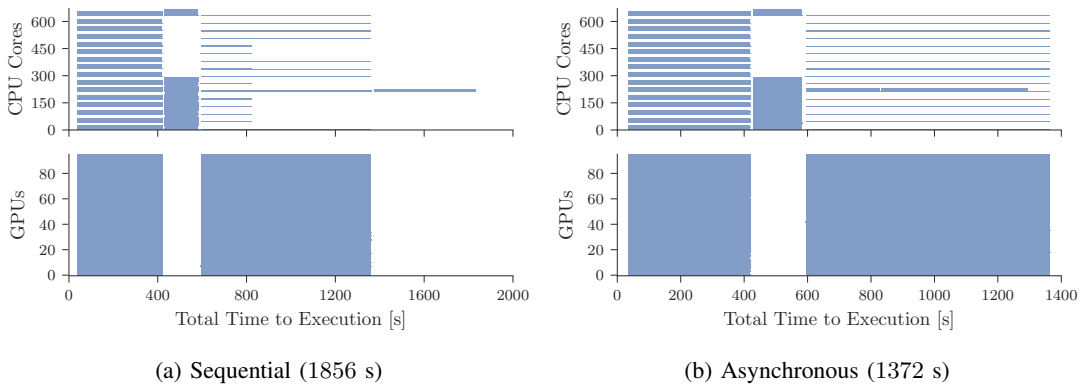


Fig. 5: Resource utilization for workflow c-DAG2. Sequential (left) and asynchronous (right) execution, with independent task sets' TTX such that  $t_{T_3, T_6} \sim t_{T_4, T_5} + t_{T_7}$ . Exploiting TX masking and the fact that sufficient resources are available, the workflow TTX is reduced by nearly 26%.

## VII. CONCLUSIONS

We have presented a study of asynchronous execution alongside an analysis of the performance impact that diverse degrees of asynchronicity have when executing workflows

with heterogeneous tasks on HPC platforms. This paper offers four main contributions: (1) an asynchronous implementation of DeepDriveMD, a framework to execute ML-driven molecular-dynamics workflows on HPC platforms at scale;

Experiment	DOA <sub>dep</sub>	DOA <sub>res</sub>	WLA	$t^{\text{Seq}}$ [s]		$t^{\text{Async}}$ [s]		$I$	
				Predicted	Measured	Predicted	Measured	Predicted	Measured
DeepDriveMD	2	1	1	1578	1707	1399	1373	0.113	0.196
c-DAG1	2	2	2	2000	1945	1972	1975	0.014	-0.015
c-DAG2	2	2	2	2000	1856	1378	1372	0.311	0.261

TABLE III: Summary of experimental results. Predicted values of  $t^{\text{Seq}}$ ,  $t^{\text{Async}}$ , and  $I$  include corrections accounting for overheads in EnTK (4%) and those incurred from enabling asynchronicity (2%) into the framework. While the degrees of asynchronicity (DOA<sub>dep</sub> and DOA<sub>res</sub>) directly determine the workflow-level asynchronicity (WLA) for a given workflow, resource utilization and task throughput, captured by the relative improvement ( $I$ ), depend on available resources and TX masking.

(2) a performance evaluation of asynchronous DeepDriveMD; (3) a model of asynchronous behavior; and (4) a general performance evaluation of that model for workflows with varying degrees of asynchronous execution.

By employing asynchronous execution in DeepDriveMD, a relative improvement  $I = 0.196$  over the sequential mode was achieved. This improvement translates to a reduction of an experimentally measured sequential TTX of 1707 s to 1372 s with asynchronicity. Two concrete workflow realizations were defined from a single arbitrary abstract DAG to demonstrate a case where the introduction of asynchronicity has a negative effect on TTX,  $I = -0.015$ , and another that gives considerable asynchronous advantage,  $I = 0.261$ . In all experiments, our model presented Sec. IV accurately predicted within less than 6% the experimentally measured values modulo framework constant overheads.

The contributions of this paper offer a first step towards the development of analytical tools for modeling the performance of workflow applications with heterogeneous tasks when executed at scale on HPC platforms. In their full maturity, those tools will allow to make *a priori* decisions about the design of both workflow runtime systems and applications, avoiding unsustainable trial and error approaches. That is a necessary precondition for the efficient and effective deployment of AI-driven workflows in production on exascale HPC platforms.

#### ACKNOWLEDGEMENTS

This work was supported by the ECP CANDLE and ExaWorks projects, the DOE HEP Center for Computational Excellence at BNL under B&R KA2401045, as well as NSF-1931512 (RADICAL-Cybertools). We thank Andre Merzky, Li Tan, and Ning Bao for useful discussions and support. We acknowledge Arvind Ramanathan, Austin Clyde, Rick Stevens and Ian Foster for useful discussions and co-development of DeepDriveMD. This research used resources at OLCF ORNL, which is supported by the Office of Science of the U.S. Department of Energy under Contract No. DE-AC05-00OR22725.

#### REFERENCES

- [1] L. Casalino, A. Dommer *et al.*, “Ai-driven multiscale simulations illuminate mechanisms of sars-cov-2 spike dynamics,” 2020.
- [2] A. Dommer, L. Casalino *et al.*, “#covidisairborne: Ai-enabled multiscale computational microscopy of delta sars-cov-2 in a respiratory aerosol,” *International Journal of High-Performance Computing Applications*, 2021.
- [3] L. Ward, G. Sivaraman *et al.*, “Colmena: Scalable machine-learning-based steering of ensemble simulations for high performance computing,” in *2021 ACM Workshop on Machine Learning in High Performance Computing Environments (MLHPC)*. IEEE, 2021, pp. 9–20.
- [4] A. Brace, I. Yakushin *et al.*, “Coupling streaming ai and hpc ensembles to achieve 100–1000× faster biomolecular simulations,” in *2022 IEEE International Parallel and Distributed Processing Symposium (IPDPS)*. IEEE, 2022, pp. 806–816.
- [5] H. Lee, M. Turilli *et al.*, “Deepdrive: Deep-learning driven adaptive molecular simulations for protein folding,” in *2019 IEEE/ACM Third Workshop on Deep Learning on Supercomputers (DLS)*. IEEE, 2019, pp. 12–19.
- [6] Q. Meng, A. Humphrey, and M. Berzins, “The uintah framework: A unified heterogeneous task scheduling and runtime system,” in *2012 SC Companion: High Performance Computing, Networking Storage and Analysis*. IEEE, 2012, pp. 2441–2448.
- [7] L. V. Kale and S. Krishnan, “Charm++ a portable concurrent object oriented system based on c++,” in *Proceedings of the eighth annual conference on Object-oriented programming systems, languages, and applications*, 1993, pp. 91–108.
- [8] H. Kaiser, T. Heller *et al.*, “Hpx: A task based programming model in a global address space,” in *Proceedings of the 8th International Conference on Partitioned Global Address Space Programming Models*, 2014, pp. 1–11.
- [9] M. Bauer, S. Treichler *et al.*, “Legion: Expressing locality and independence with logical regions,” in *SC’12: Proceedings of the International Conference on High Performance Computing, Networking, Storage and Analysis*. IEEE, 2012, pp. 1–11.
- [10] G. Bosilca, A. Bouteiller *et al.*, “Parsec: Exploiting heterogeneity to enhance scalability,” *Computing in Science & Engineering*, vol. 15, no. 6, pp. 36–45, 2013.
- [11] Y. Babuji, A. Woodard *et al.*, “Parsl: Pervasive parallel programming in python,” in *Proceedings of the 28th International Symposium on High-Performance Parallel and Distributed Computing*, 2019, pp. 25–36.
- [12] J. M. Wozniak, T. G. Armstrong *et al.*, “Swift: Scalable data flow programming for many-task applications,” in *Proceedings of the 18th ACM SIGPLAN symposium on Principles and practice of parallel programming*, 2013, pp. 309–310.
- [13] J. L. Peterson, B. Bay *et al.*, “Enabling machine learning-ready hpc ensembles with merlin,” *Future Generation Computer Systems*, vol. 131, pp. 255–268, 2022.
- [14] F. Di Natale, H. Bhatia *et al.*, “A massively parallel infrastructure for adaptive multiscale simulations: modeling ras initiation pathway for cancer,” in *Int. Conference for High Performance Computing, Networking, Storage and Analysis*, 2019, pp. 1–16.
- [15] H. Bhatia, F. Di Natale *et al.*, “Generalizable coordination of large multiscale workflows: challenges and learnings at scale,” in *Proceedings of the International Conference for High Performance Computing, Networking, Storage and Analysis*, 2021, pp. 1–16.
- [16] Y. Zamora, L. Ward *et al.*, “Proxima: Accelerating the integration of machine learning in atomistic simulations,” in *Proceedings of the ACM International Conference on Supercomputing*, 2021, pp. 242–253.
- [17] A. A. Saadi, D. Alfe *et al.*, “Impeccable: Integrated modeling pipeline for covid cure by assessing better leads,” *50th International Conference on Parallel Processing (ICPP ’21), August 9–12, 2021, Lemont, IL, USA. ACM, New York, NY, USA, 12 pages*, 2021.
- [18] A. P. Bhati, S. Wan *et al.*, “Pandemic drugs at pandemic speed: Infrastructure for accelerating covid-19 drug discovery with hybrid machine learning-and physics-based simulations on high performance computers,” *Interface Focus*.112021001820210018, 2021, <http://doi.org/10.1098/rsfs.2021.0018>.